Vol. 92 No. 5 pp. 2055–2057 ACTA GEOLOGICA SINICA (English Edition) Oct. 2018

Research Advances

Atmospheric Carbon Dioxide Reconstruction and Ocean Acidification Deduced from Carbon Isotope Variations across the Triassic–Jurassic Boundary in the Qiangtang Area, Tibetan Plateau

YI Fan[1], YI Haisheng[2,*], XIA Guoqing[2] and CAI Zhanhu[2]

1 *College of Earth Science, Chengdu University of Technology, Chengdu 610059, China*
2 *Institute of Sedimentary Geology, Chengdu University of Technology, Chengdu 610059, China*

Objective

The end-Triassic mass extinction was one of the five most profound Phanerozoic extinction events. This event was accompanied by a series of significant environmental changes, of which the most notable is the emergence of warm climate and the world-wide disappearance of carbonate platform. C isotope is one of the main means of reconstructing palaeoenvironment, however, there are very limited studies on Asia and Oceania in the East Tethys region. In China, continuous marine strata through the J/T boundary are widespread in the Qiangtang area of Tibet (Chen Lan et al., 2017), which provide us abundant research materials to study the environmental geological evolution during the T–J transition in Asian and even eastern Tethys.

Methods

The study area is located in the Qiangtang area of northern Tibetan Plateau, and the measured stratigraphic section is at the Suobucha hot spring in the Sewa region. The Upper Triassic Xiaochaka Formation consists of grey limestone, and the Lower Jurassic Quse Formation is mainly black shale. According to the previous identification of ammonites, the two formations are continuous. A total of 83 samples were collected at 2 m intervals at the T_3/J_1 boundary. And 50 micrites and argillaceous limestones were collected from the Xiaochaka Formation, and 33 calcareous shales were collected from the Quse Formation. We analyzed a total of 83 samples for $\delta^{13}C_{carb}$, $\delta^{18}O$, $\delta^{13}C_{org}$, TOC, kerogen element, $CaCO_3$ concentration and microelement. The sampling location and isotopic profiles (Appendix 1) are presented in Fig. 1

Results

The result (Appendix 1) shows that, the $\delta^{13}C_{org}$ ranges from −26.3‰ to −24.1‰, with a difference $\Delta\delta^{13}C_{org}$=2.2‰ between the maximum and minimum; $\delta^{13}C_{carb}$ ranges from −4.7‰ to −3.3‰, $\Delta\delta^{13}C_{carb}$=8‰. $\delta^{13}C_{org}$ is higher at the top of the upper Triassic Xiaochaka formation, there is a significant negative excursion between 75 and 146 m with a maximum of 2‰. The value of $\delta^{13}C_{carb}$ tends to be positive at the top of the Upper Triassic Xiaochaka Formation, and the isotopic pattern consists of two ladder-type negative anomalies between 100 and 146 m, while $\delta^{13}C_{carb}$ decrease by 3.2‰ and 7.2‰, respectively.

In recent years, oceanic surface water CO_2 concentrations have been found to be the factor controlling the $\delta^{13}C_{org}$. In addition, the CO_2 concentration at the oceanic surface is generally linked to atmospheric P_{CO2}. Rau et al. (1989) first establish a quantitative equation between marine plankton $\delta^{13}C_p$ and surface water CO_2 (a) in modern ocean. Afterwards, Fischer et al. (1998) discovered an empirical relationship between sedimentary organic matter $\delta^{13}C_{org}$ and atmospheric P_{CO2} by measuring the $\delta^{13}C_{org}$ in plankton and sedimentary organic matter in modern ocean. All these aforementioned formulas are later widely used in Quaternary paleoclimate studies and have been successfully verified by polar ice-core atmospheric P_{CO2} record. Using linear least squares methods, we applied the aforementioned formulas, global mean temperature equations and CO_2 equilibrium dissociation equations to built equations (1), (2) and (3):

$$[CO_2\,(a)]=(\delta^{13}C_{org}+14.95)/\,(-0.53) \quad (1)$$

$$\ln\,(P_{CO2})= 2.9726+1.1353\ln(CO_2(a)) \quad (2)$$

$$pH=9.6071-0.2503\ln(P_{CO2}) \quad (3)$$

Assuming that a surface seawater sample in equilibrium with the modern ocean at a salinity S=35‰, $[Ca^{2+}]$ =10.28 $mmol\cdot kg^{-1}$, carbonate saturation values Ω=5.5. The sea surface P_{CO2} and pH are shown correspondingly in Fig. 1. The results suggest that the P_{CO2} of Suobucha Section during the T–J transition range from 515 to 615 μatm. The maximum is 3.42 times to that of quaternary glaciations (P_{CO2}=180μatm) while 1.53 times to that of

* Corresponding author. E-mail: 21172210@qq.com

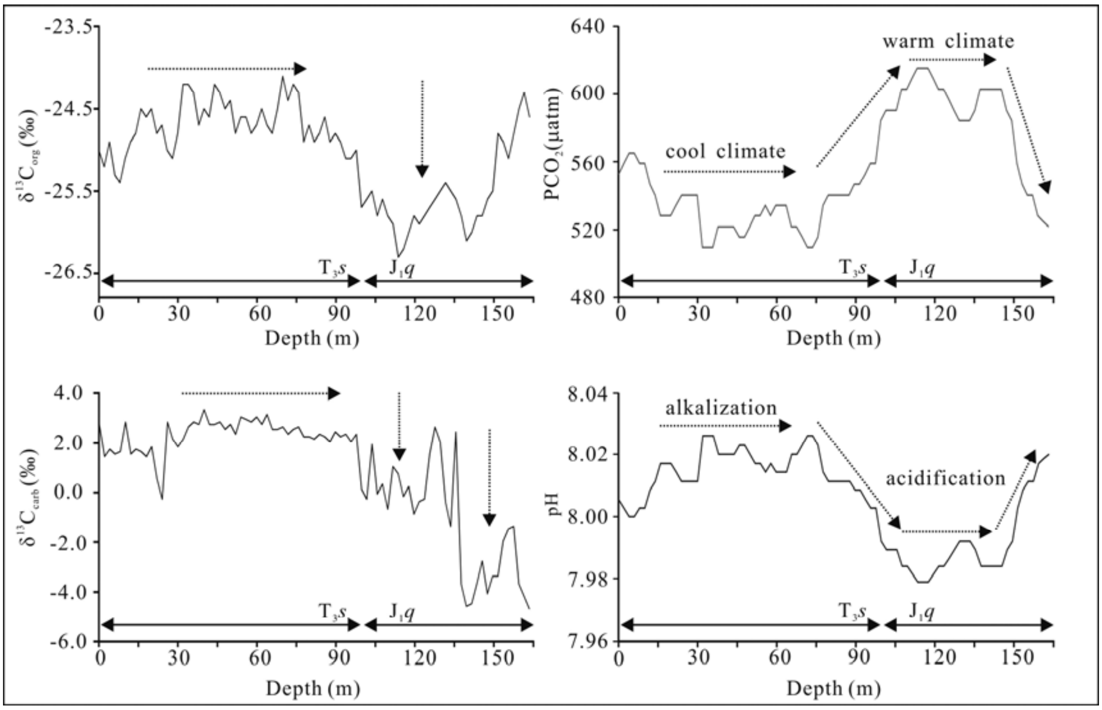

Fig. 1. Carbon isotope, P_{CO2} and pH curve of Suobucha section in the Qiangtang area.

modern (2016) global average P_{CO2} (P_{CO2}=400 μatm). High sustained P_{CO2} would result in ocean acidification. The pH valued reached its lowest 7.98, which is 0.15 lower than the modern ocean average pH 8.15.

Conclusion

In this paper, we estimate a relatively low atmospheric P_{CO2} in late Triassic and a sharp rise of P_{CO2} in early Jurassic, which leads to a conversion of cool climate into warm climate. Meanwhile, as CO_2 concentrations increase in seawater, the pH decreases and sea water acidified correspondingly. The carbonate platform sediment terminated and overlaid by the lower Jurassic argillaceous rock. The carbonate rocks were replaced by clastic rocks in stratigraphic sequence. Moreover, the increase of P_{CO2}, sea surface temperature and ocean acidification are possible reasons leading to such mass extinction.

Acknowledgments

This research was financially supported by the National Science Foundation of China (grant No. 41572089).

References

Chen Lan, Xu Guiwen, Da Xuejuan, Yi Haisheng, Zhu Zhangxiong, Huang Zhaohui and Li Xiaogang. 2017. Chemo- and biostratigraphy of the Jurassic oil shales from the Qiangtang Basin, northern Tibet, China: a case study of the Toarcian oceanic anoxic event. *Acta Geologica Sinica* (English Edition), 91(2): 630–643.

Fischer, G., Muller, P.J., and Wefer, G., 1998. Latitudinal $\delta^{13}C_{org}$ variations in sinking matter and sediments from the South Atlantic: effects of anthropogenic CO_2 and implications for paleo-P_{CO2} reconstructions. *Journal of Marine Systems*, 17(1–4): 471–495.

Rau, G.H., Takahashi, T., and Des Marais, D.J., 1989. Latitudinal variations in plankton $\delta^{13}C$: implications for CO_2, and productivity in past oceans. *Nature*, 341(6242): 516–518.

Appendix 1 Carbon isotopic values of the Suobucha section

Sample No.	Depth (m)	Isotopic value (‰)		Sample No.	Depth (m)	Isotopic value (‰)	
		$\delta^{13}C_{carb}$	$\delta^{13}C_{org}$			$\delta^{13}C_{carb}$	$\delta^{13}C_{org}$
T_3s-51	0	2.7	−25.0	T_3s-8	84	2.3	−24.8
T_3s-50	2	1.4	−25.2	T_3s-7	86	2.2	−24.6
T_3s-49	4	1.7	−24.9	T_3s-6	88	2	−24.9
T_3s-48	6	1.5	−25.3	T_3s-5	90	2.4	−24.8
T_3s-47	8	1.6	−25.4	T3s-4	92	2.2	−24.9
T_3s-46	10	2.8	−25.1	T_3s-3	94	2.3	−25.1
T_3s-45	12	1.5	−24.9	T_3s-2	96	2	−25.1
T_3s-44	14	1.7	−24.8	T_3s-1	98	2.3	−25
T_3s-43	16	1.6	−24.5	J_1q-1	100	0.1	−25.7
T_3s-42	18	1.4	−24.6	J_1q-2	102	−0.3	−25.6
T_3s-41	20	1.8	−24.5	J_1q-3	104	1.9	−25.5
T_3s-40	22	0.5	−24.8	J_1q-4	106	−0.1	−25.8
T_3s-39	24	-0.3	−24.7	J_1q-5	108	0.3	−25.6
T_3s-38	26	2.8	−25.0	J_1q-6	110	−0.7	−25.8
T_3s-37	28	2.1	−25.1	J_1q-7	112	1	−25.9
T_3s-35	30	1.8	−24.8	J_1q-8	114	0.7	−26.3
T_3s-34	32	2.1	−24.2	J_1q-9	116	−0.2	−26.2
T_3s-33	34	2.6	−24.2	J_1q-10	118	0.2	−26
T_3s-32	36	2.8	−24.3	J_1q-11	120	−0.9	−25.8
T_3s-31	38	2.7	−24.7	J_1q-12	122	−0.4	−25.9
T_3s-30	40	3.3	−24.5	J_1q-13	124	−0.3	−25.8
T_3s-29	42	2.7	−24.6	J_1q-14	126	1.5	−25.7
T_3s-28	44	2.7	−24.2	J_1q-15	128	2.6	−25.6
T_3s-27	46	2.8	−24.3	J_1q-16	130	2	−25.5
T_3s-26	48	2.5	−24.5	J_1q-17	132	−0.4	−25.4
T_3s-25	50	2.7	−24.4	J_1q-18	134	−1.4	−25.5
T_3s-24	52	2.3	−24.8	J_1q-019	136	2.4	−25.6
T_3s-23	54	3	−24.6	J_1q-020	138	−3.7	−25.8
T_3s-22	56	2.9	−24.6	J_1q-021	140	−4.6	−26.1
T_3s-21	58	2.8	−24.8	J_1q-022	142	−4.5	−26.0
T_3s-20	60	3	−24.7	J_1q-023	144	−3.7	−25.8
T_3s-19	62	2.7	−24.5	J_1q-024	146	−2.8	−25.8
T_3s-18	64	3.1	−24.7	J_1q-025	148	−4.1	−25.6
T_3s-17	66	2.5	−24.8	J_1q-026	150	−3.4	−25.5
T_3s-16	68	2.5	−24.5	J_1q-027	152	−3.4	−24.8
T_3s-15	70	2.6	−24.1	J_1q-028	154	−2	−24.9
T_3s-14	72	2.3	−24.4	J_1q-029	156	−1.5	−25.1
T_3s-13	74	2.5	−24.2	J_1q-030	158	−1.4	−24.8
T_3s-12	76	2.6	−24.3	J_1q-031	160	−3.7	−24.5
T_3s-11	78	2.2	−24.9	J_1q-032	162	−4.2	−24.3
T_3s-10	80	2.2	−24.7	J_1q-033	164	−4.7	−24.6
T_3s-9	82	2.1	−24.9				